

Etch selectivities of mask materials for micromachining of ultrananocrystalline diamond film

Byoung Su Choi^a, Jong Cheon Park^a, Sungu Hwang^b, Jin Kon Kim^b, Sung Chul Shin^c, In Won Lee^d, Jeong Ho Ryu^e, and Hyun Cho^{b,*}

^aDepartment of Nano Fusion Technology, Pusan National University, Gyeongnam 50463, Korea

^bDepartment of Nanomechatronics Engineering, Pusan National University, Busan 46241, Korea

^cNaval Architecture and Ocean Engineering, Pusan National University, Busan 46241, Korea

^dGlobal Core Research Center for Ships and Offshore Plants, Pusan National University, Busan 46241, Korea

^eDepartment of Materials Science and Engineering, Korea National University of Transportation, Chungbuk 27469, Korea

Ultra-nanocrystalline diamond (UNCD) is a very promising candidate for microelectromechanical system moving mechanical assemblies (MEMS MMAs) due to its excellent mechanical and tribological properties. In order to fabricate UNCD-based MEMS MMAs, it is important to find the mask material suitable for micromachining process. The etch characteristics of UNCD and selected mask materials (Ni, Al and SiO₂) were examined in O₂/Ar, O₂/CF₄ and O₂/SF₆ inductively coupled plasmas, and the etch selectivities of the mask materials were compared. The Ni showed very high etch selectivities to UNCD ($\geq 50 : 1$) in all three oxygen-based ICP discharges and the maximum etch selectivity of $\sim 140 : 1$ for UNCD over Ni was obtained in 100₂/5Ar ICP discharges. The Al and SiO₂ mask layers presented relatively good etch selectivities in 100₂/5Ar ICP discharges, 6.3-28.3 : 1 for UNCD over Al and 4-20 : 1 for UNCD over SiO₂, respectively. Under most of the conditions examined in 100₂/5CF₄ and 100₂/5SF₆ discharges, the Al mask showed relatively low etch selectivities of $\sim 5 : 1$ while the SiO₂ showed etch selectivities less than unity due to the extremely high volatility of SiF_x etch products.

Key words: Ultrananocrystalline diamond, Micromachining, High density plasma etching, Mask material, Etch selectivity.

Introduction

Microelectromechanical system (MEMS) has experienced a rapid growth in recent years since it provides new functionalities, space saving and cost reduction. Application fields of MEMS have continuously expanded into aerospace, automotive, telecommunications, biology, biomedicine, etc [1-5]. Most of MEMS devices are currently fabricated in silicon (Si) due to the desirable material properties and the well-established micromachining techniques with additive and subtractive processes. Si-based fully assembled MEMS devices such as electrostatic microactuators, electromagnetic micromotors and reduction gears have been fabricated using lithographic patterning and anisotropic etching techniques [6-8]. However, due to the poor mechanical and tribological properties of Si, Si-based MEMS moving mechanical assemblies (MMAs) have a limited dynamic range. For example, Si cantilever acceleration sensors and vibrational sensors are designed to avoid extensive sliding and rolling contact, and to minimize the flexural stress because of the poor flexural strength and fracture toughness of Si. Therefore, it is inevitable to find alternative materials which can implement the full potential of MEMS MMAs

even in harsh environments [9-12].

Ultrananocrystalline diamond (UNCD) is recognized as a very attractive material of choice for MEMS MMAs. UNCD films grown by CVD techniques make it possible to take advantage of excellent mechanical properties of diamond, ~ 23 times higher flexural strength and ~ 5 times greater fracture toughness compared to Si, with a very low friction coefficient less than ~ 0.1 [13-16]. In order to fabricate UNCD-based MEMS components, it is necessary to perform highly anisotropic sub-micrometer to micrometer scale micromachining into UNCD layer. Plasma etching would be the most reasonable choice for the UNCD micromachining process because of the exceptional chemical inertness of UNCD, and oxygen-based high density plasma etching has been reported to provide practical and controllable etch rates for UNCD [17-19]. A technical issue with the micromachining of UNCD is the choice of mask material since the conventional photoresists, the most widely used mask material in the plasma etching of electronic and semiconductor materials, have easily oxidizable carbon-based chemical structures and are not compatible with oxygen-based plasmas.

In this work, we report the etch characteristics of three different mask materials (silicon dioxide, nickel and aluminum) in O₂/Ar, O₂/CF₄ and O₂/SF₆ inductively coupled plasmas, and their etch selectivities to UNCD were compared to find a proper mask material for UNCD micromachining.

*Corresponding author:
Tel : +82-51-510-6113
Fax: +82-51-514-2358
E-mail: hyuncho@pusan.ac.kr

Experimental

0.5-1.0 μm thick UNCD films were deposited on (100) Si substrates of $2.5 \times 2.5 \text{ cm}^2$ area. Prior to deposition, the Si surface was textured in SF_6/O_2 inductively coupled plasmas and then ultrasonically seeded in ethanol suspension of 3-5 nm size nanodiamond particles. The UNCD films were grown in an ASTeX waveguide-equipped microwave plasma chemical vapor deposition (MPCVD) reactor using high purity CH_4 , H_2 , and Ar as the source gases. The flow rates of CH_4 , H_2 and Ar were kept constant at 4, 200 and 45 standard cubic centimeters per minute (sccm), respectively. During the deposition, process pressure and microwave power were maintained at 30 Torr and 1000 W. As-grown UNCD films were patterned with 0.1-0.2 μm thick mask layers deposited by either plasma-enhanced CVD (SiO_2) or electron beam evaporation (Ni and Al). For SiO_2 deposition, the mixtures of high purity silane (SiH_4) and nitrogen dioxide (NO_2) were used, and rf power, process pressure, and substrate temperature were maintained at 200 W, 30 Torr, and 250°C , respectively. Ni and Al mask layers were deposited at room temperature with the process pressure of 10^{-6} Torr and a very thin Cr interlayer was used to promote the adhesion between the mask layer and Si surface. High density plasma etching was performed in a planar inductively coupled plasma source operating at 13.56 MHz and with a power up to 1000 W, and the samples were thermally bonded to a Si carrier wafer that was mechanically clamped to a He backside-cooled, rf-powered (13.56 MHz, up to 450 W) chuck. O_2/Ar , O_2/CF_4 and O_2/SF_6 inductively coupled plasmas were employed to etch the UNCD films and mask layers, and the total gas load was fixed at 15 sccm. Material etch rate and etch selectivity were determined by stylus profilometry measurements and cross-sectional observation of field-emission scanning electron microscopy (FE-SEM, Hitachi S4700, operating voltage 15 kV).

Results and Discussion

Fig. 1 shows the effect of ICP source power on the UNCD and Ni etch rates (left) and the determined etch selectivity for UNCD over Ni mask layer (right) in oxygen-based inductively coupled plasmas at a low rf chuck power (200 W) and 2 mTorr pressure. The oxygen-based ICP discharges produce high and controllable etch rates for UNCD under the conditions examined. $10\text{O}_2/5\text{Ar}$ ICP discharges provide higher UNCD etch rates than $10\text{O}_2/5\text{CF}_4$ and $10\text{O}_2/5\text{SF}_6$ discharges. This is attributed to the surface bombardment effect of Ar^+ ions in the plasma increases due to the enhanced ionization reaction in the discharges, and this would increase the efficiency of physical desorption of the etch products formed on the UNCD surface [17]. $10\text{O}_2/5\text{SF}_6$ plasma produces higher UNCD etch rates than $10\text{O}_2/5\text{CF}_4$ most likely due

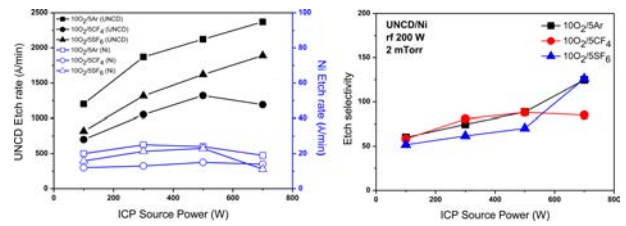


Fig. 1. UNCD and Ni etch rates (left) and etch selectivity for UNCD over Ni (right) as a function of ICP source power in $10\text{O}_2/5\text{Ar}$, $10\text{O}_2/5\text{CF}_4$ and $10\text{O}_2/5\text{SF}_6$ ICP discharges (200 W rf chuck power, 2 mTorr pressure).

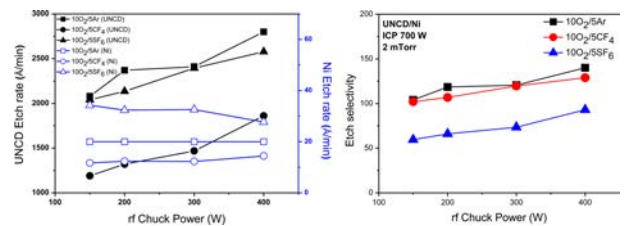


Fig. 2. UNCD and Ni etch rates (left) and etch selectivity for UNCD over Ni (right) as a function of rf chuck power in $10\text{O}_2/5\text{Ar}$, $10\text{O}_2/5\text{CF}_4$ and $10\text{O}_2/5\text{SF}_6$ ICP discharges (700 W source power, 2 mTorr pressure).

to the surface bombardments of S_xF_y species heavier than CF_x and the enhanced formation of oxyfluoride (OF^-) ions which have been reported as a highly reactive etchant for diamond [18, 20]. By sharp contrast, these oxygen-based ICP discharges produce extremely low etch rates less than $\sim 25 \text{ \AA}/\text{min}$ for Ni mask layer under the same conditions. This is ascribed to the much lower volatility of nickel oxide and nickel fluoride etch products (presumably NiO ; m.p. 1955°C , NiF_2 ; b.p. 1750°C) compared to the CO_x compounds. Consequently, Ni shows very high etch selectivities to UNCD under the conditions examined and a maximum selectivity of $\sim 126 : 1$ for UNCD over Ni is obtained in $10\text{O}_2/5\text{SF}_6$ ICP discharges.

Fig. 2 presents the influence of rf chuck power on the UNCD and Ni etch rates (left) and etch selectivity for UNCD over Ni mask layer (right) in oxygen-based inductively coupled plasmas at a fixed source power (700 W) and pressure (2 mTorr). The UNCD etch rate monotonically increases as rf chuck power increases and shows a strong dependence on the rf chuck power. This suggests that the presence of the physical component of the etching under these conditions since the average energy of energetic species bombarding the UNCD surface is generally proportional to the applied rf chuck power. The maximum UNCD etch rate of $\sim 2800 \text{ \AA}/\text{min}$ is obtained in $10\text{O}_2/5\text{Ar}$ ICP discharges at a high rf chuck power (400 W) condition. However, increasing rf chuck power does not make a significant improvement ($10\text{O}_2/5\text{Ar}$ and $10\text{O}_2/5\text{CF}_4$) or induces a slight decrease ($10\text{O}_2/5\text{SF}_6$) in Ni etch rate. In the case of Ni etching under these conditions, the average energy of energetic species increases as the rf chuck

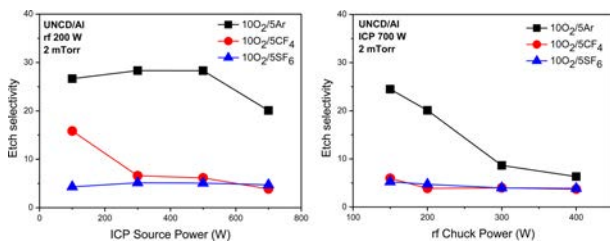


Fig. 3. Etch selectivity for UNCD over Al as a function of ICP source power (left) and rf chuck power (right) in $100\text{O}_2/5\text{Ar}$, $100\text{O}_2/5\text{CF}_4$ and $100\text{O}_2/5\text{SF}_6$ ICP discharges (2 mTorr pressure).

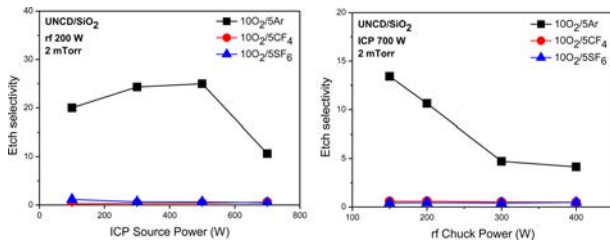


Fig. 4. Etch selectivity for UNCD over SiO_2 (right) as a function of ICP source power (left) and rf chuck power (right) in $100\text{O}_2/5\text{Ar}$, $100\text{O}_2/5\text{CF}_4$ and $100\text{O}_2/5\text{SF}_6$ ICP discharges (2 mTorr pressure).

power increases, but the flux of the reactive species in the plasma would fall down below the range of optimal values that provide sufficient oxygen or fluorine surface coverage and reaction. Therefore the etching under these conditions would be dominated by the formation of NiO_x or NiF_x etch products. Again, very high etch selectivities for UNCD over Ni are obtained and the maximum value of $\sim 140:1$ is produced in $100\text{O}_2/5\text{Ar}$ ICP discharges.

The etch selectivities of Al to UNCD in oxygen-based ICP discharges as a function of ICP source power (left) or rf chuck power (right) are shown in Fig. 3. $100\text{O}_2/5\text{Ar}$ ICP discharges produce higher etch selectivities than $100\text{O}_2/5\text{CF}_4$ and $100\text{O}_2/5\text{SF}_6$ mixtures since the addition of CF_4 or SF_6 gases to oxygen leads to the involvement of aluminum fluoride etch products (presumably AlF_3 ; m.p. 1291°C) which have higher volatility than aluminum oxide etch products (presumably Al_2O_3 ; m.p. $\sim 2000^\circ\text{C}$). $100\text{O}_2/5\text{Ar}$ ICP discharges provide relatively high etch selectivities for UNCD over Al in the range of 6.3–28.3:1 while $100\text{O}_2/5\text{CF}_4$ and $100\text{O}_2/5\text{SF}_6$ mixtures produce the etch selectivity values as low as $\sim 5:1$ under most of the conditions examined.

Fig. 4 presents the effect of ICP source power (left) and rf chuck power (right) on the etch selectivity of SiO_2 to UNCD in oxygen-based ICP discharges. $100\text{O}_2/5\text{CF}_4$ and $100\text{O}_2/5\text{SF}_6$ ICP discharges produce very low selectivities less than $\sim 1:1$ under most conditions examined since these two fluorine-containing oxygen discharges produce the SiO_2 etch rates higher than those of UNCD due to the extremely high volatility of SiF_x etch products (presumably SiF_4 ; b.p. -86°C). This result clearly shows that the SiO_2 is not a desirable mask material for the micromachining of UNCD layer

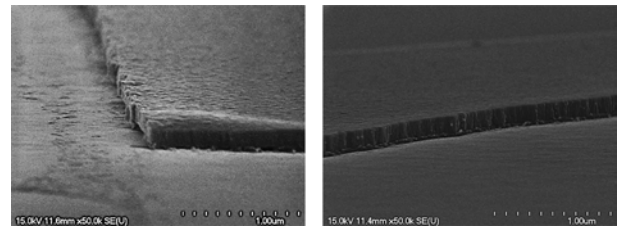


Fig. 5. SEM micrographs of features etched into UNCD using $100\text{O}_2/5\text{Ar}$ ICP discharges (700 W source power, 400 W rf chuck power, 2 mTorr pressure).

using O_2/CF_4 and O_2/SF_6 ICP etching. On the contrary, SiO_2 shows the etch selectivity to UNCD ranged from 4.1:1 to 20:1 in $100\text{O}_2/5\text{Ar}$ ICP discharges due to much lower volatility of silicon oxide etch products (presumably SiO_2 ; b.p. 2230°C) than the SiF_x compounds.

Fig. 5 shows FE-SEM micrographs of features etched into UNCD films using $100\text{O}_2/5\text{Ar}$ ICP discharges with a relatively high source power (700 W) and high rf chuck power (400 W) condition which produced the highest etch rate of $\sim 2800 \text{ \AA}/\text{min}$ for UNCD as shown in Fig. 2. In each case, a very thin Ni film with thickness of $\sim 100 \text{ \AA}$ was used as the mask layer and was removed in a mixed acidic solution composed of H_3PO_4 , HNO_3 , CH_3COOH and DI water (volume ratio of 3:3:3:1) after etching. Etch depth of the UNCD layer was maintained at $\sim 2000 \text{ \AA}$. Due to the very high etch selectivity of $\sim 140:1$ under this condition, as shown in Fig. 2, it is very clear that the Ni mask layer provided a very good protection to keep the underlying UNCD layer from the physical and chemical interactions with the reactive species in the $100\text{O}_2/5\text{Ar}$ ICP discharges. The etched UNCD surface shows a smooth surface morphology and a highly anisotropic pattern transfer was performed.

Conclusions

The etch characteristics of UNCD and selected mask materials (Ni, Al and SiO_2) were investigated in oxygen-based (O_2/Ar , O_2/CF_4 and O_2/SF_6) inductively coupled plasmas, and the etch selectivities of the mask materials were compared to find a suitable mask material for micromachining of UNCD. Practical and controllable UNCD etch rates were obtained in all three plasma chemistries and the UNCD etch rate showed a strong dependence on the ICP source power and rf chuck power under the conditions examined. The maximum UNCD etch rate of $\sim 2800 \text{ \AA}/\text{min}$ was obtained in $100\text{O}_2/5\text{Ar}$ ICP discharges at a high rf chuck power (400 W) condition. Ni showed excellent etch selectivities higher than $\sim 50:1$ under the conditions examined due to the low volatility of potential etch products (NiO and NiF_2) and the surface chemical reaction-limited etch mechanism. The maximum etch selectivity of $\sim 140:1$ was obtained in $100\text{O}_2/5\text{Ar}$ ICP

discharges. For the Al mask layer, 10O₂/5Ar ICP discharges produced higher etch selectivities than 10O₂/5CF₄ and 10O₂/5SF₆ discharges because of the higher volatility of aluminum fluoride etch products compared to aluminum oxide compounds. The SiO₂ showed relatively good etch selectivities in 10O₂/5Ar ICP discharges, but 10O₂/5CF₄ and 10O₂/5SF₆ discharges produced extremely low etch selectivities less than ~ 1 : 1 due to the very high volatility of SiF_x etch products. Among the three mask materials studied in this work, Ni would be the best mask material which can provide an excellent protection to UNCD in the process of sub-micrometer to micrometer scale micromachining for the fabrication of UNCD-based MEMS MMAs.

Acknowledgments

This work was supported by the National Research Foundation of Korea (NRF) grant funded by the Korea government (MSIP) through GCRC-SOP (No. 2011-0030013).

References

1. H. Qu, *Micromachines* 7 (2016) 14-35.
2. N.F. de Rooij, S. Gautsch, D. Briand, C. Marxer, G. Mileti, W. Noell, H. Shea, U. Staufer and B. van der Schoot, in *Proceedings of IEEE Transducers 2009*, June 2009 Denver, USA, p.17.
3. T. James, M.S. Mannoer, and D.V. Ivanov, *Sensors* 8 (2008) 6077-6107.
4. J. Bryzek, S. Roundy, B. Bircumshaw, C. Chung, K. Castellino, J.R. Stetter, and M. Vestel, *IEEE Circuits & Dev. Magazine* March/April (2006) 8-28.
5. S. Kon, K. Oldham, and R. Horowitz, *Proc. SPIE* 6529 (2007) 65292V-1~65292V-11.
6. S.M. Spearing, *Acta Mater.* 48 (2000) 179-196.
7. J.W. Judy, *Smart Mater. Struct.* 10 (2001) 1115-1134.
8. R. Bogue, *Sensor Rev.* 27 (2007) 7-13.
9. A.P. Lee, A.P. Pisano, M.G. Lim, *Mater. Res. Soc. Proc.* 276 (1992) 67-70.
10. K.J. Gabriel, F. Behi, R. Mahadevan, M. Mehregany, *Sensors and Actuators A* 21-23 (1990) 184-188.
11. M.N. Gardos, in "Tribology Issues and Opportunities in MEMS", Kluwer Scientific Publishers, edited by B. Bushan (1998) 341.
12. L. Tong, M. Mehregany, L.G. Matus, *Appl. Phys. Lett.* 60 (1992) 2992-2994.
13. R.K. Ahmad, A.C. Parada, S. Hudziak, A. Chaudhary and R.B. Jackman, *Appl. Phys. Lett.* 97 (2010) 093103-1~093103-3.
14. E. Chevallier, E. Scorsone, H.A. Girard, V. Pichot, D. Spitzer and P. Bergonzo, *Sensors and Actuators B* 151 (2010) 191-197.
15. A.R. Krauss, O. Auciello, D.M. Gruen, A. Jayatissa, A. Sumant, J. Tucek, D.C. Mancini, N. Moldovan, A. Erdemir, D. Ersoy, M.N. Gardos, H.G. Busmann, E.M. Meyer and M.Q. Ding, *Diamond & Related Mater.* 10 (2001) 1952-1961.
16. W.H. Liao, D.H. Wei and C.R. Lin, *Nanoscale Res. Lett.* 7 (2012) 82-89.
17. J.C. Park, S.H. Kim, S.U. Cha, O.G. Jeong, T.G. Kim, J.K. Kim and H. Cho, *J. Nanosci. Nanotechnol.* 14 (2014) 9078-9081.
18. J.C. Park, S.H. Kim, T.G. Kim, J.K. Kim, B.W. Lee and H. Cho, *Modern Phys. Lett. B* 29 (2015) 1540022-1~1540022-5.
19. H. Uetsuka, T. Yamada and S. Shikata, *Diamond & Related Mater.* 17 (2008) 728-731.
20. K.J. Sankaran, S. Kunuku, S.C. Lou, J. Kurian, H.C. Chen, C.Y. Lee, N.H. Tai, K.C. Leou, C. Chen, and I.N. Lin, *Nanoscale Res. Lett.* 7 (2012) 522-527.